Journal of Cleaner Production 236 (2019) 117604

Contents lists available at ScienceDirect

Journal of Cleaner Production

journal homepage: www.elsevier.com/locate/jclepro

A probabilistic approach for determining the influence of urban traffic management policies on energy consumption and greenhouse gas emissions from a battery electric vehicle

Roberto Álvarez Fernández*, Sergio Corbera Caraballo, Francesc Clar López

Department of Industrial Engineering, Antonio de Nebrija University, Pirineos 55, 28040, Madrid, Spain

ARTICLE INFO

Article history:
Received 15 March 2019
Received in revised form
5 July 2019
Accepted 9 July 2019
Available online 13 July 2019

Handling Editor: Zhifu Mi

Keywords:
Battery electric vehicle
GHG emissions
Energy consumptionprediction
Route information
Speed profile

ABSTRACT

Drivers appear to be in control of all factors affecting vehicle performance. However, they are still subject to following traffic rules. These may be regulations like prohibitions or warnings, such as speed limits, or actions required by traffic control such as traffic lights and stop signs, that randomly influence the vehicle speed profile while driving. Driving behavior has an undeniable impact on vehicle greenhouse gas emissions, either from a tailpipe or in the form of indirect emissions resulting from charging batteries with electricity from the grid, and is a milestone for successful decarbonization of road transport. In this study, the authors propose a probabilistic approach to reaffirm and evaluate the influence of traffic management conditioning factors on driving behavior, energy consumption, and greenhouse gas emissions of a battery electric vehicle in a city. A Stochastic Route Speed Profile was developed based on the stochastic behavior of route elements affecting vehicle energy consumption. In this approach, the route rather than the driver, is analyzed for constraints and limitations that randomize energy consumption and air emissions. Human influence on driving behavior becomes irrelevant when route driving obligations are decisive. This probabilistic approach suggests an alternative view for understanding and evaluating the environmental impacts of traffic control decisions or urban planning regulations in terms of their effects on routes and their characteristics. A case study is presented for a route in Madrid, reflecting variations in vehicle energy consumption up to 70 Wh/km for a set of proposed scenarios with varying the number and performance of traffic lights.

© 2019 Elsevier Ltd. All rights reserved.

1. Introduction

Since its beginning over one hundred years ago, with the Model T, to the present day, on-road transport contributions to greenhouse gas (GHG) emissions have been steadily rising, such that today these emissions, along with diminishing air quality, represent a serious problem not only for the largest cities but for the global environment (Woodcock et al., 2009).

The transport sector is responsible for emitting 7,737.8 million tonnes of carbon dioxide equivalent (CO_{2eq}).[1] As noted in Fig. 1, this represents 24% of GHG worldwide emissions, of which 5,792 million tonnes comes from on-road transport (IEA. International Energy Agency, 2017). This problem is caused by the strong dependence on cars in the largest cities and the historical absence of sustainable mobility proposals. Some measures have been taken since the Kyoto Protocol agreement (1992), which were intensely reinforced during the Paris Climate Conference (2015), to reduce emissions. However, the demand for transport has continued to grow for the principal reason that more passengers and freight loads are traveling because of population growth, production and consumption (Qi et al., 2018). The growth of consumption in commodities and services has increased a set of activities related to progress and social welfare that play a major role in the metabolism of cities. Control and reduction of emissions in the housing, transport and logistics sectors (Fathollahi-Fard and Hajiaghaei-Keshteli, 2018) must be prioritized by policymakers to coordinate all these activities to reduce energy consumption at the minimum cost (Fu et al., 2019). The aim is to minimize effects on climate change, air pollution and traffic congestion (Govindan et al., 2015)(Liu et al.,

* Corresponding author.
E-mail address: ralvarez@nebrija.es (R.Á. Fernández).

[1] Carbon dioxide equivalency describes, for a given amount of GHG, the corresponding amount of CO_2 that would achieve the same Global Warming Potential (GWP) when it is measured over a specified timescale (100 years) (IEA. International Energy Agency, 2017).

https://doi.org/10.1016/j.jclepro.2019.117604
0959-6526/© 2019 Elsevier Ltd. All rights reserved.

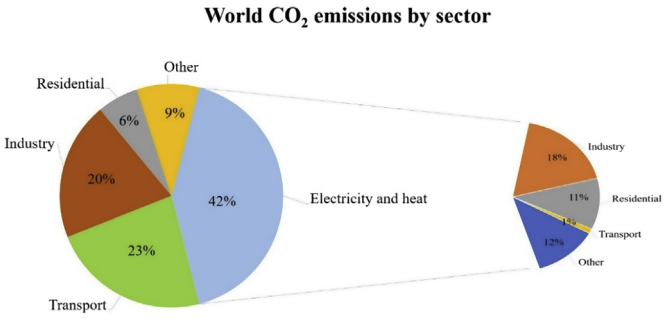

Fig. 1. Greenhouse gas emissions by economic sector.

2019)(Aguado et al., 2013) without sacrificing drivability or pedestrian protection. This is not an easy task, because progressive world population growth (in 2015 the population was 7.35 billion and will be 9.157 by 2040), can be quickly translated to mean higher energy requirements for sustaining enhanced living standards (Jones and Warner, 2016) (Fathollahi-Fard et al., 2018) (Fathollahi-Fard et al., 2019).

Some of the aforementioned measures needed to curb GHG emissions have focused on improving the Internal Combustion (IC) powertrains (O'Driscoll et al., 2018), or introducing mitigation techniques (Sepehri and Sarrafzadeh, 2018) which can substantially reduce the risks associated with human-induced global warming (González-Mahecha et al., 2019). Other measures have included emphatic restrictions for heavy polluters and privileged access for low-emitting vehicles in sensitive areas. Both Madrid (Borge et al., 2018) and London (Transport for London, n.d.), not only reduced the number of vehicles, but also promoted zero emission mobility through tax exemptions or subsidizing the purchase of alternative vehicles and fuels at the expense of traditional fossil fuels. The Spanish government, through the Movea and Movalt schemes, has set aside 20 million euros for grants for the purchase of electric and gas-fueled cars (IDAE, 2018).

This new framework has been the starting point for promoting the Battery Electric Vehicle (BEV) as the greatest contributor to GHG and air pollution abatement (Ensslen et al., 2016). Consequently, if the electric transport is the new mobility paradigm, it is absolutely necessary to consider, not only well-known BEV market barriers (She et al., 2017) including the range anxiety[2] phenomenon, but also development of tools to analyze and improve how the vehicle is driven, because this is one of the most influential factors for vehicle energy consumption. It is true that although performance of the vehicle will mainly depend on driver behavior (Alvarez et al., 2015) (Fernández, 2018) and traffic congestion (Papageorgiou et al., 2003) (Greenwood et al., 2007), cities still impose a set of constraints beyond driver control such as pedestrian crossings, traffic lights, speed limits, roundabouts, and bus stops (Ferreira and D'Orey, 2012) (Munoz-Organero et al., 2018) (Coelho et al., 2005) (SARTRE consortium, 2004). These constraints can affect the number of starts and stops and vehicle speed. This inevitably creates uncertainty about the proportion of fuel consumption while driving that depends on driver decisions. With internal combustion vehicles this uncertainty represents a significant instantaneous environmental problem of greenhouse gas emissions and air quality, but for battery electric vehicles the problem is worse, since it combines the environmental aspect (often neglected) with the lack of confidence in electric transport (Junquera et al., 2016).

City-conditioned driving directly impact travel itineraries choices with the aim of minimizing energy consumption, environmental impacts (eco-driving and eco-routing) or travel times. However, Palat et al. (2014) published the results of a questionnaire-based study showing that, at driver decision-making level, routes with fewer traffic lights were preferred even if the probability of having to stop at those lights were high and waiting times at the red lights were long. This individual preference could sometimes cause non-optimal route choices from the environmental perspective. To reduce fuel consumption and emissions, tactical decisions like urban planning or traffic regulations as well as operational decisions like driving behavior must be considered (Coloma et al., 2017) at the public administration level of decision-making. The traffic data collection necessary to propose appropriated travel itineraries for minimizing fuel consumption and associated environmental impacts (Sivak and Schoettle, 2012) must consider speed, geographic data, travel times and fuel consumption, among others.

Therefore, the author's goal for this work is to establish a simplified method for visualizing the influence of city constraints (urbanism, laws, traffic regulation elements) on the energy consumption and consequent GHG emissions of a BEV on a given route. The main contribution of this work is the methodology developed to build a speed cycle for a concrete route, where the influence of human behavior is minimized, in such a way that the vehicle specifically obeys to road constraints, passenger safety, comfort and city regulations. This could be a useful tool for urban planners to improve understanding of the influence of traffic control infrastructure and other regulations on energy consumption and GHG emissions.

This paper is organized as follows: the methodology is explained in the second section in three main blocks: energy basis, probability basis and calculation possibilities. In the third section the method is applied to a real route in Madrid. The following sections present the discussion of results, conclusions, and the need for future research.

2. Energy consumption estimation approach

The aim of this research is to develop a method that explains the influence of city traffic control rules on energy consumption of a BEV. This section describes the basis of the proposed approach, in order to enhance prediction of energy consumption inherent to a route when a BEV is driven using a simple and computationally efficient way. The authors focused on energy consumption because the relationship between electricity and GHG emissions is straightforward (Álvarez et al., 2015). The section is divided in three subsections: the first explains the importance of route characterization considering the elements affecting vehicle driving and energy consumption. The second explores the fundamentals of calculating route-associated energy. The third subsection explains how to manage uncertainty surrounding the calculation.

2.1. Route modelling for enhancing energy consumption prediction

The proposed method is based on the discretization of the route, which starts with its subdivision in a set of basic entities called stretches. The approach aims to simplify the evaluation of all route constraints that play a crucial role in predicting BEV energy consumption. In this sense, and in terms of route characterization, the energy consumption is defined as the sum of individual consumptions associated with basic actions of driving each stretch that constitute what the authors call the Stochastic Route Speed Profile (SRSP).

[2] Worry of a person driving an electric car that the battery will run out of power before the destination or a suitable charging point is reached (Rauh et al., 2015).

When discrete math is applied for modelling any real system or phenomenon, among all the parameters involved, the size of the basic entities (the length of stretches in the case of a route) is positioned as one of the most relevant aspects when determining the final results. In this study, the authors have defined the stretch length according to two aspects related to the driving procedure: maximum allowed speed and the assumption that, to save energy, city driving is based on two basic driving actions:

a) The driver operates at maximum speed allowed because no stop requirement is encountered.
b) The driver stops the car as a consequence of a route requirement and, after the stop event ends, the driver accelerates the vehicle until reaching the maximum speed allowed.

Both basic driving actions are influenced by the city regulations and traffic control elements. The proposed discretization corresponds to a stochastic speed profile for the route, defined as a combination of the basic driving actions covering the whole route. This SRSP is highly dependent on the maximum speed allowed and on the probability of stop requirements. In order to obtain the SRSP linked to a route it will be necessary to subdivide the route in a concrete number of stretches, therefore, it is necessary to define a standard stretch length. Analyzing the two basic driving actions, it is easy to understand that the first implies a sum of times and distances, namely: (1) the distance necessary to stop the vehicle due to a traffic event, starting from the maximum legal speed allowed and (2) the distance until reaching the maximum speed limit of the road again. This sum of distances is defined as the basic stretch length and depends on the maximum speed allowed and positive or negative accelerations. Notably, the stopping action must not cause harm to vehicle occupants, therefore deceleration and acceleration values must be selected accordingly. For example, safe travelling stopping distance from a maximum speed limit of 50 km/h is 25 m according to the Spanish Directorate General of Traffic (DGT) (DGT, 2018). It implies that a constant deceleration/acceleration of 3.9 m/s^2 would be understandable.

Once the basic stretch length is calculated, it is possible to subdivide the route into a concrete number of stretches where the two aforementioned basic driving profiles would be combined, subject to compliance with the maximum speed allowed. However, it is possible to find different speed limits along the length of a specified route. Thus, the mathematical representation of the route will not be composed by a sole stretch length value, but there will exist as many values as different maximum speeds along the route. Denoting p as the number of changes of maximum speeds allowed in a route, and k as the number of maximum different speeds, the discretization into stretches will be constructed by a set of these elements with different baseline lengths Lv_i with $i = 1, \ldots, k$ (see Equation (1)). In relation to the number of stretches of each length, Nv_i, this number geometrically depends on the route length, L, and its composition of stretch lengths, Lv_i. According to this and from the speed point of view, the route can be modelled as a set of stretches grouped in k subsets, each of them with Nv_i, and Lv_i as reference values, comprising Equation (1).

$$L = \sum_{i=1}^{k} N_{vi} \cdot L_{vi} \tag{1}$$

In order to improve predictions of energy consumption, a route cannot only be characterized by the speed limits for each stretch, but must also consider the aforementioned basic driving actions. Two driving actions are considered when driving each stretch to assign the energy consumption: the obligation to stop or not. For each stretch of a specified speed limit, the two aforementioned driving behavior options are:

- Option one (O_1): Drive at the maximum speed allowed for the length of the stretch.
- Option two (O_2): Stop from maximum allowed speed to zero due to traffic event and, stopping, accelerate to the maximum speed allowed. In this case, it will be assumed that:
  - the speed zero will always take place in the middle of the stretch and
  - the acceleration and deceleration are constant values.

A new driving behavior option is also included:

- Option three (O_3): Accelerate/brake from the maximum speed allowed to the following.

With this basis, each of the k subsets is composed of several stretches (Nv_i) where the behavior can adopt the O_1 or O_2 option. Therefore, the stretches associated with a speed and clustered into a corresponding subset are denoted as:

- mv_i for stretches of type O_1 associated to a speed limit vi and hence with a Lvi length.
- nv_i for stretches of type O_2 associated to a speed limit vi and hence with a Lvi length.

With $mv_i = 0 \ldots Nv_i$, $nv_i = 0 \ldots Nv_i$ and subject to Equation (2):

$$N_{vi} = m_{vi} + n_{vi} \tag{2}$$

The SRSP resulting from the discretization of the route is based on different k speed limits, causing the appearance of several breaks, p, in the continuity of the speed profile along the route length, which affects energy consumption. However, this implies the necessity of a new type of basic driving action: speed adjustment between two different maximum allowed and consecutive speeds (v_i and v_j). For energy calculation, v_i and v_j are considered the initial and final speeds of a uniform motion in a straight line, where the acceleration or deceleration of the vehicle is assumed constant. This can be reflected in the route characterization in one of two ways:

- The route representation must include p additional stretches called *transition stretches* and denoted as t_i. These stretches are considered a new driving action type (O_3) which is represented by new defined stretches whose lengths must be calculated and added using Equation (1), to obtain Equation (3).

$$L = \sum_{i=1}^{p} L_{ti} + \sum_{i=1}^{k} N_{vi} \cdot L_{vi} \tag{3}$$

- Transition stretches can be intended as offline transitions for achieving continuity between consecutive stretches with different speed limits. This implies energy consumption in some circumstances and energy recovery in others. This energy is considered in the overall energy report, but it is not necessary to define new stretches because it is assumed that the energy is either consumed or recovered in previous and future stretches.

In summary, according to the assumptions, a route can be expressed as an assemblage of basic entities called stretches which, according to their definition, allow us to characterize the topology in terms of speed limit and possible driving actions, creating a

probabilistic driving cycle. The stretches are clustered in k subsets (S_1 … S_k) as a function of their speed limit. Each subset includes several stretches (Nv_i); each is classified as mv_i or nv_i in accordance with the corresponding driving behavior (O_1 or O_2) options. Additionally, there is a set of p transition stretches to explain the variations of speed from one subset to another. The route definition can be mathematically expressed as:

$$R_t = \{S_1 \cup S_2 \cup \ldots \cup S_K\} \cup T_{rt} \tag{4}$$

being:

$$S_1 = \{m_{v1,1}, m_{v1,2} \ldots, m_{v1,Nv1}\} \cup \{n_{v1,1}, n_{v1,2} \ldots, n_{v1,Nv1}\} \tag{5}$$

$$S_2 = \{m_{v2,1}, m_{v2,2} \ldots, m_{v2,Nv2}\} \cup \{n_{v2,1}, n_{v2,2} \ldots, n_{v2,Nv2}\}$$

$$\vdots$$

$$S_k = \{m_{vk,1}, m_{vk,2} \ldots, m_{vk,Nv1}\} \cup \{n_{vk,1}, n_{vk,2} \ldots, n_{vk,Nvk}\}$$

$$T_{tr} = \{t_1, t_2, \ldots, t_p\}$$

where T_{tr} represents the transition stretches, each S_k represents the vector of characteristics (behaviour, subset position, presence) and each $m_{v_i,j}$, tj and $n_{v_i,j}$ takes value 1 or 0 within the subset to represent:

- The type of driving action (m implies O_1, n implies O_2 and t implies O_3).
- Maximum speed associated with subset v_i.
- The position within the route (stretch j).
- The existence of m or n in stretch j is the criteria for assigning values of 1 or 0.

Finally, substituting the terms in Equation (4), a route can be represented by a vector $\boldsymbol{R_t}$ in the form expressed in Equation (6), defined as the characteristic route vector, which includes all necessary information for addressing the energy consumption according to some level of uncertainty.

$$\begin{aligned}\boldsymbol{R_t} = &\{m_{v1,1}, m_{v1,2} \ldots, m_{v1,Nv1}\}, \{m_{v2,1}, m_{v2,2} \ldots, m_{v2,Nv2}\}, \\ &\{m_{vk,1}, m_{vk,2} \ldots, m_{vk,Nv1}\}, \{n_{v1,1}, n_{v1,2} \ldots, n_{v1,Nv1}\}, \\ &\{n_{v2,1}, n_{v2,2} \ldots, n_{v2,Nv2}\}, \{n_{vk,1}, n_{vk,2} \ldots, n_{vk,Nvk}\}, \{t_1, t_2, \ldots, t_p\}\end{aligned} \tag{6}$$

Then,

$$m_{vi} = 0 \ldots \sum_{j=1}^{Nvk} m_{v_i,j} \text{ and } n_{vi} = 0 \ldots \sum_{j=1}^{Nvk} n_{v_i,j}$$

must accomplish Equation (2).

Fig. 2 shows a graphical representation of the SRSP and characteristic vector $\boldsymbol{Rt_A}$ of route A with two maximum speed limits (k = 2).

$$R_{tA} = \{\{1,0,1,0,1,0\}; \{0,0,0,0,1,0,0\}; \{0,1,0,0,0,1\}; \{0,0,0,0,0,0\}; \{1,1\}\}$$

$p = 2;\ k = 2;\ Nvk = 6;\ mv_1 = 3;\ mv_2 = 1;\ nv_1 = 2;\ nv_2 = 0.$

2.2. Stretch energy consumption determination

All the formulas necessary to calculate the energy associated with the vehicle driving actions O_1, O_2 and O_3 are explained in this section. Each defined stretch contains specific parameters which have a direct impact on the energy consumption of a BEV. These are:

- Maximum speed limit.
- Length of stretch.
- Basic driving actions.

Other parameters necessary for calculating the energy consumption, such as road elevation or air density, can be obtained from tools like Google Maps or Open Street Map (Haklay and Weber, 2008). Equation (7) represents the general formula used to quantify the energy consumption in 1 s of vehicle operation, CP_{BEV} (kWh), that has been proposed in previous studies (Alvarez et al., 2015).

$$CP_{BEV} = M \cdot v \cdot a + \frac{1}{2} \cdot \rho \cdot C_D \cdot A \cdot v^3 + M \cdot g \cdot h + \tau \cdot M \cdot g \cdot v \tag{7}$$

Most of these factors are not random, but rely on human factors or political decisions that have a certain randomness.

Discretizing the route into stretches, the energy consumption for a given stretch can be calculated by applying well-known vehicle dynamics (7). Evidently, this equation must be adapted for each driving action and is susceptible to simplification. Values for gravity and air density are considered constant due to the imperceptible changes that can take place within a city. The elevation term in many cases is assumed to be zero because the altitude variation of altitude can be disregarded to reduce computational cost. Therefore, energy consumption ultimately depends on driving actions (Zubelzu and Álvarez, 2016) (Álvarez et al., 2015), which in this case are randomly conditioned to a stretch and can variously be O_1, O_2 or O_3 type. Consequently, the energy consumption will be different for each case.

Nonstop stretches (type O_1) are governed by Equation (8) for energy evaluation, where v represents the maximum speed allowed in this stretch and acceleration is equal to zero.

$$CP_{BEV}(constant\ speed) = \frac{1}{2} \cdot \rho \cdot C_d \cdot A \cdot v^3 t + M \cdot g \cdot v \cdot t \cdot \tau \tag{8}$$

The driving profiles type O_2 stretches are divided into two actions:

- The first action is the deceleration from initial speed (maximum allowed) to zero. It can be calculated the energy that can be recovered and returned to the battery. However, this energy may or may not be considered in the final report because it is difficult to know the percentage of braking energy that is actually recovered, as recovery depends on regenerative braking effectiveness (Lv et al., 2015), and this information is usually unavailable. Braking energy follows Equation (9):

$$\begin{aligned}CP_{BEV}(braking) = \int_0^t P(t)dt = \int_0^t F(t) \cdot v(t)dt = \int_0^t \Big[&-(M \cdot a) \\ &+ \left(\frac{1}{2} \cdot \rho \cdot C_d \cdot A \cdot v(t)^2\right) + (M \cdot g \cdot \tau)\Big] \cdot v(t)dt\end{aligned} \tag{9}$$

$$v(t) = v_0 - a \cdot t$$

where v represents the maximum speed allowed and t represents the braking time.

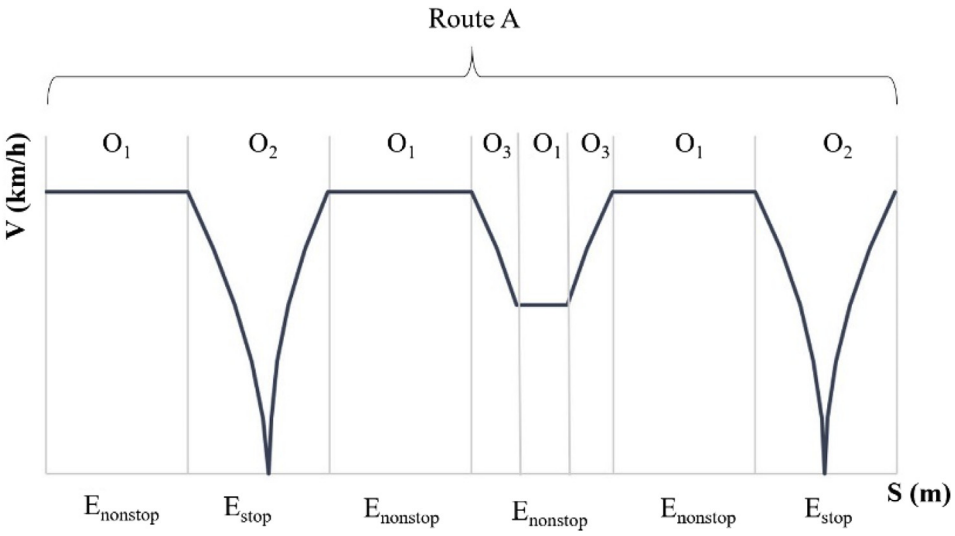

Fig. 2. Scheme of the SRSP for a route, displaying subsets, stretches and driving actions.

- The second action of the O_2 type stretch corresponds to vehicle acceleration from zero to the maximum speed limit with constant acceleration. In this case, energy is calculated by applying Equation (10), where v represents maximum speed allowed and t represents acceleration time.

$$CP_{BEV}(accelerating) = \int_0^t P(t)dt = \int_0^t F(t)\cdot v(t)dt = \int_0^t \left[M\cdot a + \left(\frac{1}{2}\cdot\rho\cdot C_d\cdot A\cdot v(t)^2\right) + (M\cdot g\cdot\tau)\right]\cdot v(t)dt \quad (10)$$

$$v(t) = a\cdot t$$

Finally, O_3 stretches represent the transition from a maximum speed value in a specific stretch to another maximum speed value defined by the contiguous stretch. This transition can imply acceleration or deceleration depending on the speed variation, and Equations (9) (10) allows us to obtain the value of CP_{BEV} (*trans*).

As previously mentioned, the main differentiating factor among energy consumption for each stretch is related to the driving behavior (O_1, O_2 and O_3). Stretches with the same speed limit will consume the same energy only if they share the same driving profile. In terms of energy consumption, stretches sharing both speed limit and driving action can be merged because they consume the same amount of energy. This reduces calculation time, since consumption for a given route depends only on the number and type of the stretches. To more efficiently compute energy evaluation and data manipulation, the energy consumption of the route (E_T) can be calculated based on the matrix format:

$$E_T = M_s\cdot M_e \quad (11)$$

where $\boldsymbol{M_s}$ is a row array created from the route characteristics vector, $\boldsymbol{R_t}$, by grouping those stretches that share maximum speed and driving behavior, and $\boldsymbol{M_e}$ is a column array that contains both the energies associated with each stretch type for a given speed corresponding to transition stretches.

$$M_s = \{m_{v1}, m_{v2}, \ldots, m_{vk},\ n_{v1}, n_{v2}, \ldots, n_{vk},\ t_1, t_2, \ldots, t_p\} \quad (12)$$

where,

$$m_{vi} = 0\ldots\sum_{j=1}^{Nvk} m_{v_i j} \text{ and } n_{vi} = 0\ldots\sum_{j=1}^{Nvk} n_{v_i j}$$

and:

$$\boldsymbol{M_e} = \begin{Bmatrix} E_{mv1} \\ E_{mv2} \\ \vdots \\ E_{mvk} \\ E_{nv1} \\ E_{nv2} \\ \vdots \\ E_{nvk} \\ E_{t1} \\ E_{t2} \\ \vdots \\ E_{tp} \end{Bmatrix} \quad (13)$$

The result of the scalar product ($\boldsymbol{M_s}\cdot\boldsymbol{M_e}$) of these is the overall energy consumption E_T. This value can increase if the consumption of accessory loads such as lights, air conditioning or radio is considered. The use of air conditioning, for example, increases fuel consumption by up to 20% (Ehsani et al., 2018).

2.3. Uncertainty basis explained

The evaluation of energy consumption when a BEV drives a determined route cannot be considered a deterministic process. In the route representation described in Section 2.1, there are two decision levels that can clearly be distinguished in defining topology (characteristic vector): the creation of the subsets must be subjected to the speed limit, and within each subset the classification of the inner stretches must attend to the associated driving action. The range of allowable speed limits is intrinsically linked to a route, therefore the number of subsets, transitions and their dimensions are characteristic and unambiguous for a given route. In this sense, it can be affirmed that the topology characterization of a route based on speed is a deterministic process. On the other hand,

the driving profile topology associated with each subset, and consequently the route (SRSP), is strongly influenced by external inputs which, can be considered random by the route mathematical model of energy consumption. External inputs are subject to probabilistic laws and are responsible for stretch changes from O_1 to O_2. Therefore, the parameters m_{vk} and n_{vk} are influenced by probabilities. Consequently, the prediction of energy consumption for a given route must be treated as a probabilistic model subject to a set of probabilities for occurrence of external inputs affecting the driving actions within each stretch. It is apparent that the characteristic vector of a route, as stated in Equation (6), only summarizes the stretch's composition in order to calculate the consumption of a concrete energy as a function of the driving profile. However, it does not provide information about the distribution of different m_{vk} and n_{vk} along the route length. When the energy consumption does not depend on random factors, stretches and their driving profile distributions are not required, but in this case, as consequence of the randomness of external inputs and the methods used to obtain stretch length, each stretch has only one probability, (P_i), that a stop action is not required and the vehicle can run along the stretch without stopping, sustaining the maximum allowed speed. Consequently, there is a complementary probability *(1-P_i)* that a stop action is required. This implies that a probabilistic study to obtain the values of R_t and the probability of this sequence of events needs to be conducted. The probabilistic study results would be strongly influenced by each P_i value as well as stretch positions associated with this probability. However, it is impossible not to assume that uncertainties around driving actions as a consequence of the stopping probability are random and independent of driver decision.

To efficiently perform this study, the authors propose breaking down the route into a new set of topology entities called sub-routes. The concept of sub-route refers to a portion of the route which clusters all consecutive stretches between two transition stretches. It represents an intermediate level between the route and the stretch. According to the sub-route conception criteria, each route can be divided into *p+1* sub-routes based on the number of speed limit changes, *p*, between consecutive stretches. Its modelling is consistent with discretization basics and route representation. Thus, each sub-route is represented by a characteristic row vector in the form of Equation (14):

$$Sb_p = \{\{m_{vi,p,1}, m_{vi,p,2}\ldots, m_{vi,p,r}\}, \{n_{vi,p,1}, n_{vi,p,2}\ldots, n_{vi,p,s}\}\} \tag{14}$$

Where p is the identification of the sub-route, $m_{v_i,p,1}$, $m_{v_i,p,2}$, …,$m_{v_i,p,r}$ represent the O_1 stretches distribution and $n_{v_i,p,1}$, $n_{v_i,p,2}$, …, $n_{v_i,p,s}$ corresponds to the O_2 type. The overall energy consumption and probability of the route can be now expressed as the combination of different sub-routes. The energy is obtained by the sum of the consumption of the included sub-routes while the probability is calculated as the product of the probabilities defined for each sub-routes (as each sub-route is an independent event). The sub-route concept involves modifications, and is structured in two stages such that its resolution can be conducted in the easiest and most computationally efficient manner. This means:

- First stage: Evaluating the probability of occurrence of each driving behavior sequence that is feasible in each sub-route. All possible stop and nonstop events that may occur while the vehicle is driving along the sub-route are included in the driving behavior sequences.
- Second stage: Conducting the possible variations of driving behavior sequences associated with each of the different sub-routes to predict overall energy consumption and its associated.

The proposed method is conceived as a map of occurring events. Random driving options of each sub-route are connected, and a set of energy consumptions is obtained where each is linked to the probability of its occurrence. The columns of Fig. 3 correspond to each sub-route, while the rows show the variety of feasible driving behavior sequences. The data contained in the blocks refer to the number of $m_{v_i,p,r}$ and $n_{v_i,p,s}$ (events sequences), their energy consumption, and the probability of occurrence each sub-route, respectively.

For the two stages shown in Fig. 3, probabilities are presented for each sub-route (determining its own probability of occurrence) as well as for the combination of all sub-routes, resulting in a map of all possible energy consumption and probabilities. From a probabilistic point of view, each sub-route is independent; therefore, as the probability of two or more independent events occurring together can be determined by multiplying individual probabilities, probabilities of all available sub-routes that comprise a complete route can be obtained.

The probability of each string of events included in a sub-route will depend on the number of stretches, the probability of stops or nonstops inherent to each one and the feasible combinations of $\{m_{v_i,p,1}, m_{v_i,p,2}, \ldots, m_{v_i,p,r}\}$ and $\{n_{v_i,p,1}, n_{v_i,p,2}, \ldots, n_{v_i,p,s}\}$. In mathematical notation, the number of feasible events combinations can be expressed as a sum of permutations (15):

$$\sum_{i=0}^{Sgr} PR_{Sgr}^{i,\ Sgr-i} \tag{15}$$

Which must accomplish a consistency constraint:

$$dim\{m_{vi,p,1}, m_{vi,p,2}\ldots, m_{vi,p,r}\} + dim\{n_{vi,p,1}, n_{vi,p,2}\ldots, n_{vi,p,s}\} = S_{gr} \tag{16}$$

where S_{gr} is the number of stretches that make up the corresponding maximum speed v_i sub-route. Expression (15) allows us to determine the exact number of sequences for which the probabilistic study should be performed. Concerning the probability that a sequence of stop and nonstop events could take place in a concrete sub-route (same number of $m_{v_i,p,r}$ and $n_{v_i,p,s}$), the calculation addresses the probability of combining multiple events (Ross, 2018) through Equation (17).

$$P(A_1 \cup A_2 \cup \ldots \cup A_n) = P\left(\sum_{k=1}^{n} P(A_k) - \sum_{\substack{i,j=1 \\ i<j}}^{n} P(A_i \cap A_j) + \sum_{\substack{i,j,k=1 \\ i<j<k}}^{n} P(A_i \cap A_j \cap A_k) + \ldots + (-1)^{n+1} \cdot P(A_1 \cap A_2 \cap \ldots \cap A_n)\right) \tag{17}$$

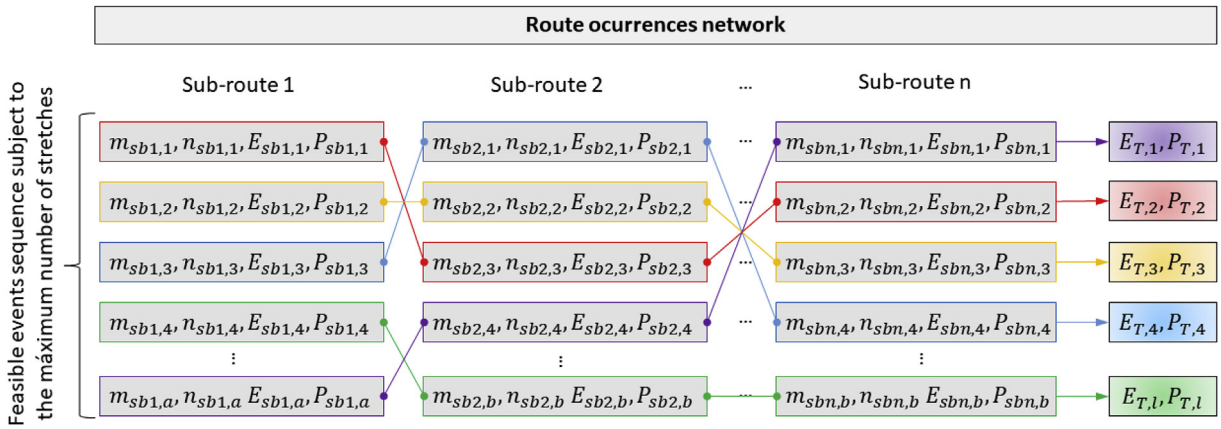

Fig. 3. Map of occurring events.

In Equation (17),[3] A_i represents a random combination of stretch events which show the topology of stop and nonstop events in a sub-route. The number of A_i events for each sequence results from different variations of the stretch positions (O_1 type and O_2 type) within a specific sub-route. This value is directly related to the number of stretches that compose the sub-route and the number of permutations of the $m_{v_i,p,r}$ and $n_{v_i,p,s}$ events which define each sequence. Thus, the number of cases can be conceived as the permutation of $m_{v_i,p,r}$ and $n_{v_i,p,s}$ along the number of stretches of the sub-route. Regarding the probability of combined events, this is when the role of the sub-route becomes apparent, since grouping consecutive stretches with the same speed limit results in the same number of $m_{v_i,p,r}$ and $n_{v_i,p,s}$ having the same respective energy consumption. This issue is particularly relevant from a computational efficiency point of view, because once the sub-route is defined, the energy consumption for each feasible sequence is immediately obtained, and only the probabilities require further attention.

Consequently, in the sub-route context the probability associated with energy consumption is equivalent to the probability that a sequence of stop and nonstop events can take place.

$$Ec_{sbi} = m_{v_i,p} \cdot E_{mv_i} + n_{v_i,p} \cdot E_{nvi} \tag{18}$$

being:

$$m_{vi,p} = dim\{m_{vi,p,1}, m_{vi,p,2}, \ldots m_{vi,p,r}\} \text{ and } n_{vi,p} = dim\{n_{vi,p,1}, n_{vi,p,2}, \ldots n_{vi,p,s}\}$$

In a matrix format, the aforementioned equation implies that each sub-route has an associated a set of arrays (M_{sbc}, M_{sbr} and M_{sbn}), with the following characteristics:

- Two columns representing the energy associated with a sequence of stop and nonstop events and its resulting probability.
- A number of rows r obtained by applying $\sum_{i=0}^{Sgr} PR_{Sgr}^{i,\ Sgr-i}$.

The purpose of M_{sbc} is to resume the different energy consumptions and their probabilities inherent to a sub-route as a result of the number of feasible driving sequences and their probabilities. Notably, the probability located in each row of M_{sbc} is obtained (19).

Once each sub-route is defined, the number of cases in each sequence, as well as the matrix M_{sbc} dimension, are automatically initialized and the process can be computationally implemented.

In parallel with M_{sbc} (which represents energy consumption) M_{sbr} is built, the matrix which accounts for allowable recovery energy in the sub-route because of regenerative braking (stop action in stretches O_2 and speed reduction action in stretches O_3) and driving downhill. If the capacity of the powertrain to recover energy (α) is known, it can generate a final matrix M_{sbn}, which includes the net energy consumption in the sub-route (19).

$$M_{sbn} = M_{sbc} - \alpha \cdot M_{sbr} \tag{19}$$

Finally, once the occurrence probability of each feasible driving behavior sequence in each sub-route is evaluated, the overall energy consumptions and their assigned probabilities can be predicted (second stage), computing the possible combinations between the driving action sequences associated with each of the different sub-routes. In this sense, the overall energy can be expressed by the following sum of consumptions:

$$E_{ROUTE} = \sum_{i=1}^{p+1} E_{SUB-ROUTEi} + \sum_{i=1}^{p} E_{transition\ i} \tag{20}$$

$$P(E_{ROUTE}) = \prod_{i=1}^{p+1} P(E_{SUB-ROUTEi}) \tag{21}$$

To illustrate the proposed approach, Fig. 4 represents a route with seven stretches and two maximum allowed speeds, v_1 and v_2. The sequence of speeds allows for the stretches to be grouped into two sub-routes (Sb_1 and Sb_2) separated by a transition stretch. In each stretch, there are three possible driving actions, the energy associated to each, and the probability of occurrence. These values can be initialized for the following data for each sub-route:

- The number of feasible sequences to be analyzed in terms of energy and occurrence probability according to Expression (15) and constraint (16):

$$\sum_{i=0}^{Sgr} PR_{St}^{i,\ Sgr-i} = 4$$

$$dim\{m_{v1,p,1}, m_{v1,p,2}, m_{v1,p,3}\} + dim\{n_{v1,p,1}, n_{v1,p,2}, n_{vi,p,3}\} = 3$$

where $p = 1$ for Sb_1 and $p = 2$ for Sb_2

[3] Equation (17) will be simplified by eliminating the probabilities of intersections, in so far as the event is incompatible with all the others, therefore the probability of intersection would be equal to zero, reducing Equation (17) to the term $\sum_{k=1}^{n} P(Ak)$.

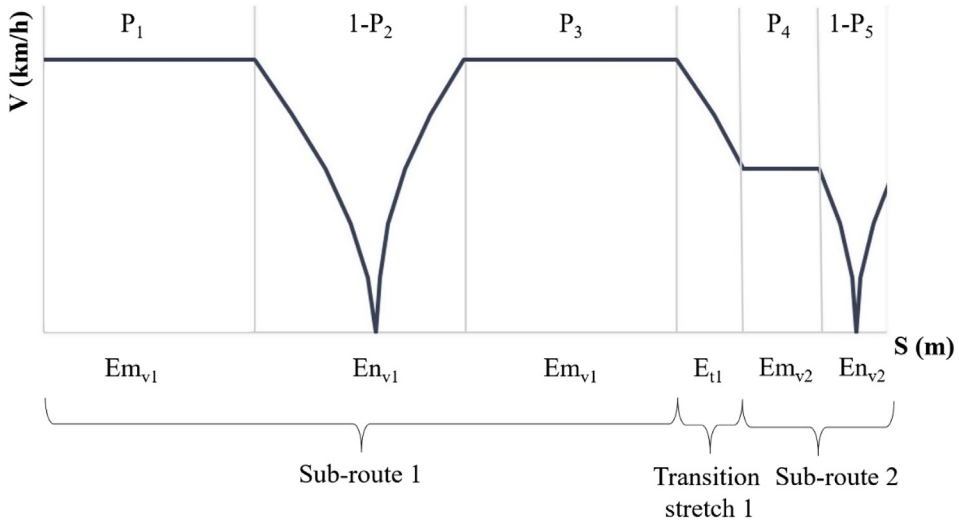

Fig. 4. Example of a driving cycle for a route with two sub-routes.

- The energy consumption associated with each feasible sequence of stretch and event combinations for each sub-route: $Ec_{sb,m,n}$

$$Ec_{sb,m,n} = m_{v_1,1} \cdot E_{mv_1} + n_{v_1,1} \cdot E_{nv1}$$

$$m_{v_1,1} = 0\ldots3; n_{v_1,1} = 0\ldots3$$

$$m_{v_1,1} + n_{v_1,1} = 3$$

- The number of cases for each specific sequence of stop and nonstop events for conducting the probability of occurrence. Using permutations involves consideration of event positions within the sub-route.

With these data, a calculation tree is built to obtain the energy and overall probability for each sequence of each sub-route (see Fig. 5). As both sub-routes apply the same method, the authors will only explain the operations tree for Sb_1.

Finally, the M_{sbc} matrix is obtained for each sub-route:

$$M_{sbc1} = \begin{Bmatrix} Ec_{sb1,1,1} & P_{sb1,1,1} \\ Ec_{sb1,1,2} & P_{sb1,1,2} \\ Ec_{sb1,1,3} & P_{sb1,1,3} \\ Ec_{sb1,1,4} & P_{sb1,1,4} \end{Bmatrix}$$

Parallel to the M_{sbc} matrix (which covers the energy consumption) is the M_{sbr} matrix, which is composed of all the energy that can theoretically be recovered by a vehicle in each stretch of the sub-route and which does not affect the probability of the sub-route.

$$M_{sbr1} = \begin{Bmatrix} Er_{sb1,1,1} & 0 \\ Er_{sb1,1,2} & 0 \\ Er_{sb1,1,3} & 0 \\ Er_{sb1,1,4} & 0 \end{Bmatrix}$$

Finally, the M_{sbn} matrix is created that includes the net energy consumption if the energy recovery capacity of the powertrain α is known, following the equation:

Sequences $\{m_{v_1,1}\ n_{v_1,1}\}$	Energy	Overall Probability	Cases
{3,0}	$Ec_{sb1,1,1}$	$P_{sb1,1,1} = P(A_1)$	$A_1 = \{m_{v_1,p,1}, m_{v_1,p,2}, m_{v_1,p,3}\}$ $P(A_1) = p_1 \cdot p_2 \cdot p_3$
{2,1}	$Ec_{sb1,1,2}$	$P_{sb1,1,2} = P(A_1 \cup A_2 \cup A_3)$	$A_1 = \{n_{v_1,p,1}, m_{v_1,p,2}, m_{v_1,p,3}\}$ $P(A_1) = (1-p_1) \cdot p_2 \cdot p_3$ $A_2 = \{m_{v_1,p,1}, n_{v_1,p,2}, m_{v_1,p,3}\}$ $P(A_2) = p_1 \cdot (1-p_2) \cdot p_3$ $A_3 = \{m_{v_1,p,1}, m_{v_1,p,2}, n_{v_1,p,3}\}$ $P(A_3) = p_1 \cdot p_2 \cdot (1-p_3)$
{1,2}	$Ec_{sb1,1,3}$	$P_{sb1,1,3} = P(A_1 \cup A_2 \cup A_3)$	$A_1 = \{n_{v_1,p,1}, n_{v_1,p,2}, m_{v_1,p,3}\}$ $P(A_1) = (1-p_1) \cdot (1-p_2) \cdot p_3$ $A_2 = \{n_{v_1,p,1}, m_{v_1,p,2}, n_{v_1,p,3}\}$ $P(A_2) = (1-p_1) \cdot p_2 \cdot (1-p_3)$ $A_3 = \{m_{v_1,p,1}, n_{v_1,p,2}, n_{v_1,p,3}\}$ $P(A_3) = p_1 \cdot (1-p_2) \cdot (1-p_3)$
{0,3}	$Ec_{sb1,1,4}$	$P_{sb1,1,4} = P(A_1 \cup A_2 \cup A_3)$	$A_1 = \{n_{v_1,p,1}, n_{v_1,p,2}, n_{v_1,p,3}\}$ $P(A_1) = (1-p_1) \cdot (1-p_2) \cdot (1-p_3)$

Fig. 5. Calculation of energies and associated uncertainties.

$$M_{sbn} = M_{sbc} - \alpha \cdot M_{sbr} = \begin{Bmatrix} Ec_{sb1,1,1} - \alpha \cdot Er_{sb1,1,1} & P_{sb1,1,1} \\ Ec_{sb1,1,2} - \alpha \cdot Er_{sb1,1,2} & P_{sb1,1,2} \\ Ec_{sb1,1,3} - \alpha \cdot Er_{sb1,1,3} & P_{sb1,1,3} \\ Ec_{sb1,1,4} - \alpha \cdot Er_{sb1,1,4} & P_{sb1,1,4} \end{Bmatrix}$$

2.4. Route energy consumption calculation

This method provides a probabilistic map of the energy consumed by a BEV linked to a given route and subjected to road events. This information can be analyzed from different points of

view, for example, an assessment of the potential risk of range anxiety that the drivers experience when driving the route beginning with a concrete State of Charge (SoC). Another point of view is that of fleet energy management, such as a car-sharing business or a last-mile delivery company. Efficient vehicle management (e.g. minimizing charging inactivity times) would be cost-effective for such a company. Additionally, potential energy savings would be reflected in reduced indirect GHG emissions.

To estimate the route energy consumption and its associated uncertainty, the procedure first obtains the probability distributions by applying the method to all sub-routes comprising the overall route. Matrix M_{sbc} or matrix M_{sbn} will be used to construct the probability framework, where each M_{sbc} corresponding to each sub-route generates a random discrete variable GC_{sb} or NC_{sb} for Gross or Net Consumption, respectively, that is composed of r values obtained in M_{sbc} or M_{sbn} and their corresponding probabilities. Equation (22) shows the structure of the NC_{sb}.

$$NC_{sb} = \begin{cases} En_{sb,i,1} & P(NC_{sb} = En_{sb,i,1}) \\ En_{sb,i,2} & P(NC_{sb} = En_{sb,i,2}) \\ \vdots & \vdots \\ En_{sb,i,r} & P(NC_{sb} = En_{sb,i,r}) \end{cases} \quad (22)$$

where r elements are ranked in increasing order. Each random discrete variable represents the probability of occurrence of this energy net consumption value, where:

$$\sum_{i=1}^{r} P(\mathrm{NCsbi}) = 1 \quad (23)$$

The set of random discrete variables (one for each sub-route) allows for evaluation of different scenarios of consumption and probability. Each random discrete variable is characterized by its mean $E(NC_{sb})$ and variance $Var(NC_{sb})$, which represents the expected value of the squared deviation from the mean. In order to explain consumption, this must be defined as the random variable NC_{route} that represents the sum of all sub-route discrete random variables NC_{sb}. In this sense, the Central Limit Theorem (CLT) (Ross, 2018) (Alvarado and Batanero, 2006) is applied to assign a normal distribution in Equation (24).

$$NC_{route} \rightarrow N\left(\sum_{i=1}^{r} E(NC_{sbi}),\ \sqrt{\sum_{i=1}^{r} \mathrm{Var}(NC_{sbi})}\right) \quad (24)$$

Once the energy is defined for the overall random route, the method ends when transition stretches are considered. These stretches are not subject to probability and the net consumption/generation only affects the mean of NC_{route}. Thus, it can be added at the end of calculations, according to the properties of normal distribution (Ross, 2018).

$$NC_{route} \rightarrow N\left[\left(\sum_{i=1}^{r} E(NC_{sbi}) + \sum_{i=1}^{p} Et_i,\ \sqrt{\sum_{i=1}^{r} \mathrm{Var}(NC_{sbi})}\right)\right] \quad (25)$$

where the term $\sum_{i=1}^{p} Et_i$ represents the consumption/generation of transition stretches.

In the following Section 3, a route of the city of Madrid (Spain) is evaluated to explore the versatility and flexibility of this method.

3. Application to a real route in the city of madrid

To apply the proposed methodology, a route in Madrid was selected and the influence of the constraints on energy consumption and emissions were studied.

Fig. 6 shows a picture of the route (closed loop, 3.25 km length, indicating the starting point and endpoint (1)). There are two maximum allowed speeds, v1 = 50 km/h (13.89 m/s) and v2 = 30 km/h (8.33 m/s), four changes of maximum speed (four transition stretches) and five sub-routes. Table 3 shows the results of applying route discretization and energy consumption. Sub-routes are individually analyzed to generate their arrays of energy and probabilities. In this route these elements represent only traffic lights and the following values were used: 0.4 (nonstop) and 0.6 (stop) for sub-routes one, three and five while 0.2 (nonstop) and 0.8 (stop) have been used for sub-routes two and four, respectively, to simplify the calculation. Those stretches with no uncertainly events (traffic lights in this case) assumed a stop probability of zero.

The vehicle selected for energy consumption calculation was a Renault Zoe. The main characteristics of its vehicle dynamics (Renault, 2018) are reflected in Table 1.

As it can be seen in Fig. 6, the complete route is subdivided into five sub-routes and four transition stretches. The complete information is detailed in Table 2.

For each sub-route, the mean, expected value, and the variance of the random variable $E(NC_{sbi})$ and $Var(NC_{sbi})$, respectively, are presented.

Sub-route 1	$E(NC_{sb1}) = 26$ Wh	$Var(NC_{sb1}) = 210.5$ W^{2}h^2
Sub-route 2	$E(NC_{sb2}) = 102$ Wh	$Var(NC_{sb2}) = 113.9$ W^{2}h^2
Sub-route 3	$E(NC_{sb3}) = 213$ Wh	$Var(NC_{sb3}) = 1{,}263$ W^{2}h^2
Sub-route 4	$E(NC_{sb4}) = 144$ Wh	$Var(NC_{sb4}) = 190$ W^{2}h^2
Sub-route 5	$E(NC_{sb5}) = 22$ Wh	$Var(NC_{sb5}) = 210.5$ W^{2}h^2

When the CLT is applied, a normal distribution representing the consumption of energy (in Wh) is obtained for the route.

$$NC_{route}(Wh) \rightarrow N\left(\sum_{i=1}^{r} E(NC_{sbi}),\ \sqrt{\sum_{i=1}^{r} \mathrm{Var}(NC_{sbi})}\right) = \boldsymbol{N}(508,\ 44)$$

The energy consumed/generated in the transition stretches can be considered a fixed energy consumption/generation and can therefore be added at the end, considering the properties of the normal distribution.

$$E_t = \sum E_{ti} = 43\ Wh$$

Obtaining the final value for the normal distribution assigned to the NC random variable:

$$NC_{route}(Wh) \rightarrow \boldsymbol{N}(551,\ 44)$$

Once the overall energy consumption value is estimated by applying a discrete variable approach and its approximation to a normal distribution applying the CLT is established, it is possible to compare all possibilities of energy consumption by applying combinatory rules. This approach is based on building the route through all possible combinations of sub-routes as the complete route is the intersection of a set of independent sub-routes that compose a complete route. The energy consumption for each combination of sub-routes is the sum of the energy of each sub-

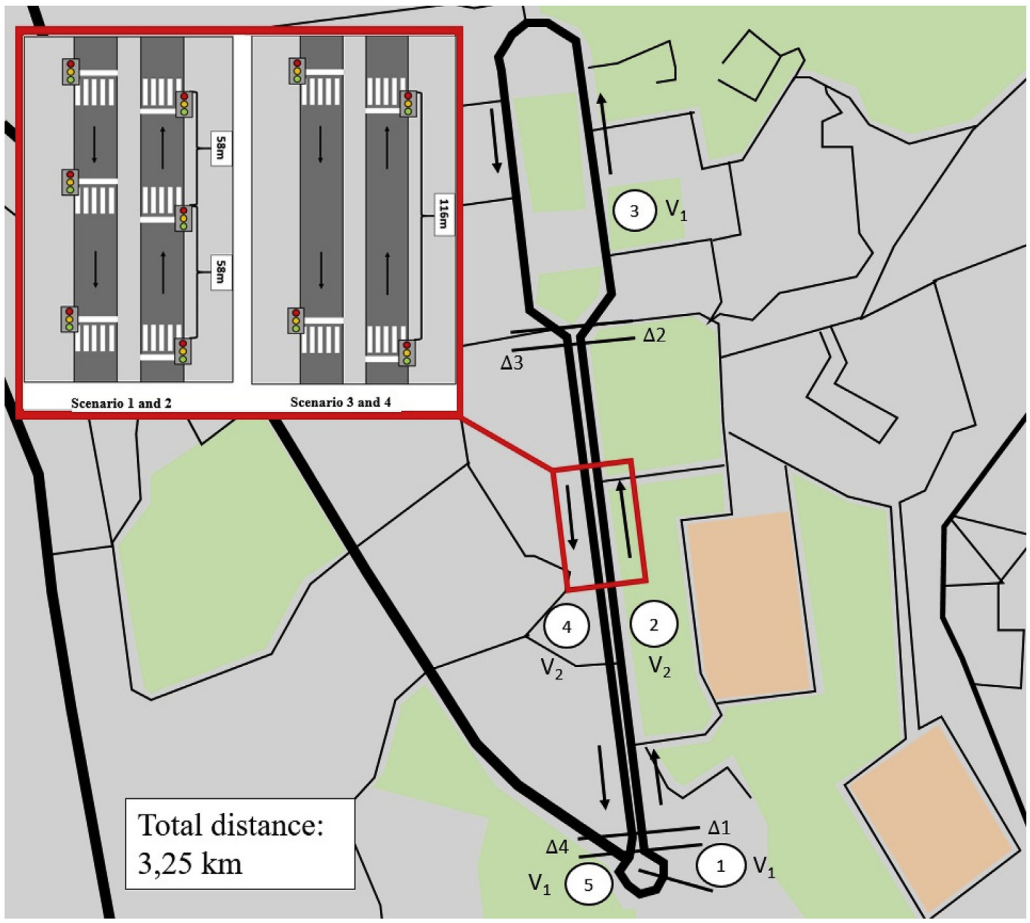

Fig. 6. Route overview.

Table 1
Vehicle dynamics specifications.

Parameter	Symbol	Value
Vehicle mass (kg)	M	1,450
Frontal area (m^2)	A	2.71
Aerodynamic resistance coefficient	C_d	0.34
Energy recovery coefficient (%)	α	0.2
Rolling resistance coefficient	τ	0.013
Static friction coefficient	μ	0.6
Road angle (°)	Φ	0
Air density at 20 °C (kg/m^3)	ρ	1.204
Gravity (m/s^2)	g	9.81

route, and the probability of occurrence is the product of the probabilities of each included sub-route. Once calculated and sorted in increasing order of energy consumption, a histogram was built with twenty classes, 20.56 Wh wide, and the class boundary for the histogram was selected such that all classes had the same width. The plotted results approximate a normal (Fig. 7) distribution N **(550.9, 44.67)**.

This result confirms the valuable approximation of the first method.

The expected value given by the normal distribution provides clear information for users to establish comparison between routes or when planning different consumption scenarios assuming lower or higher risk levels to run out of battery. In example, if the route selected were driven without taking into account the stop events (traffic lights off), the vehicle would achieve a net consumption of 270 Wh, which implies 84 Wh/km, lower than the 133 Wh/km obtained by following the Commission Directive 93/116/EC (The Commission of the European Communities, 2013), which in turn is lower than 170 Wh/km estimated when the traffic lights are working.

According to the properties of the normal distribution, within the interval [462, 640] (Wh) 95% of probabilities are concentrated (Alvarado el al, 2005), which explains the distribution N **(551, 44)**. Therefore, this implies an interval with the most probable consumption [142, 197] in Wh/km. On the other hand, if the driver is forced to stop at every traffic light, the consumption could reach 680 Wh (210 Wh/km). It is evident that the differences observed were clearly due to the number of uncertain events and their (random) influence on vehicle performance, causing variations in energy consumption.

4. Results and discussion

To illustrate the influence on consumption and emissions caused by policymaker decisions, the methodology is applied in a set of four scenarios summarized in Table 3. Comparing Scenarios 1 and 2 or Scenarios 3 and 4 reflects the influence of variation in the maximum allowed. Scenarios 2 and 3 represent the present situation and Scenario 1 and 4 represent actual past situations. Scenarios 3 and 4 show variations in consumption and emissions when the number of stop events is varied.

Fig. 6 details the locations of six traffic lights. Their performance was decided in the past mainly to facilitate pedestrian crossing

Table 2
Sub-route information.

Sub-route 1	Value
Maximum allowed speed (m/s)	13.89
Length of stretch (m)	50
Total number of sub-route stretches	2
Number of stretches with uncertainty	1
Energy stretch type O_1 (Wh)	4.2
Energy stretch type O_2 (Wh)	41.3
Energy recovered by stretch O_2 (Wh) ($\alpha = 20\%$ applied)	7.6
Transition stretch 1	**Value**
Length (m)	16
Energy recovered by stretch type O_3 (Wh) ($\alpha = 20\%$ applied)	4.8
Sub-route 2	**Value**
Maximum allowed speed (m/s)	8.3
Length of stretch (m)	18
Total number of sub-route stretches	44
Number of stretches with uncertainty	6
Energy stretch type O_1 (Wh)	1.1
Energy stretch type O_2 (Wh)	14.8
Energy recovered by stretch *O2* (Wh) ($\alpha = 20\%$ applied)	2.8
Transition stretch 2	**Value**
Length (m)	16
Energy stretch type O_3 (Wh)	26.5
Sub-route 3	**Value**
Maximum allowed speed (m/s)	13.89
Length of stretch (m)	50
Total number of sub-route stretches	26
Number of stretches with uncertainty	6
Energy stretch type O_1 (Wh)	4.1
Energy stretch type O_2 (Wh)	41.3
Energy recovered by stretch O_2 (Wh) ($\alpha = 20\%$ applied)	7.6
Transition stretch 3	**Value**
Length (m)	16
Energy recovered by stretch type O_3 (Wh) ($\alpha = 20\%$ applied)	4.8
Sub-route 4	**Value**
Maximum allowed speed (m/s)	8.33
Length of stretch (m)	18
Total number of sub-route stretches	50
Number of stretches with uncertainty	10
Energy stretch type O_1 (Wh)	1.1
Energy stretch type O_2 (Wh)	14.8
Energy recovered by stretch O_2 (Wh) ($\alpha = 20\%$ applied)	2.8
Transition stretch 4	**Value**
Length (m)	16
Energy stretch type O_3 (Wh)	26.5
Sub-route 5	**Value**
Maximum allowed speed (m/s)	13.89
Length of stretch (m)	50
Total number of sub-route stretches	1
Number of stretches with uncertainty	1
Energy stretch type O_1 (Wh)	4.1
Energy stretch type O_2 (Wh)	41.3
Energy recovered by stretch O_2 (Wh) ($\alpha = 20\%$ applied)	7.6

without regard for their impact on fuel consumption and emissions. Scenarios 3 and 4 represent a situation in which four of the elements have been deactivated (the distance between the central traffic light and the other two is 58 m).

To quantify the impact of proposed regulatory options on consumption and emissions, it is necessary to estimate the number of vehicles circulating along the route every day. This zone is considered "fluid traffic", which means there is a density of 100–500 vehicles per hour (Ayuntamiento de Madrid, 2019), which can be estimated at nearly 6000 vehicles/day. The conversion of electricity consumption (kWh) and the corresponding GHG emissions ($kgCO_2eq$) is established using the information provided about the mix of electricity sources in Spain (ElectricityMap, 2019).

To highlight the influence of variations caused by the traffic control elements, the route selected had only traffic lights with the same stopping probability for each. Fig. 8 summarizes the results. Each group of bars corresponds to the emissions of the four scenarios applying the same probability of stopping (starting from 0.1) to all traffic light elements on the route. That information allows us to see the influence of the regulation of the green and red periods of traffic lights, which caused an upward trend in all the scenarios, linked to increasing the probability of vehicle stopping from 0.1 to 0.9. It can also be observed that the minimum variation in Scenario 1 versus 4 and Scenario 2 versus 3 was due to the variation in the number of traffic lights. Only when the probability of stopping had significant variation were differences apparent. However, the speed variation from 50 km/h to 30 km/h caused a notable variation in emissions between Scenarios 1 and 4 and Scenarios 2 and 3.

Another interesting result was that Scenario 1 and Scenario 4 emitted equivalent carbon dioxide when stopping probability was low (0.1 and 0.2) to Scenario 2 and Scenario 3 when stopping probability was higher (0.8 and 0.9). This shows that two different measures (variation of the allowed speed and variation in the number of traffic lights) could cause similar or different results in emissions by changing the management of traffic light performance. This circumstance also occurs in the real world.

With these scenarios, the authors have tried to demonstrate that the location of traffic control elements and circulation rules impact the consumption of energy and variations in GHG emissions. This simplified model shows that urban transformation must consider the effects of the aforementioned elements and others that cause similar effects (e.g. pedestrian crossing, stop signals, bus stops, roundabouts) will be studied and included in future models.

Although other factors, such as traffic jams and driving behavior, influence consumption, the analysis of the route itself provides relevant information for:

- Urban policymakers, allowing them to foresee emissions consequences when planning urban transformations.
- Last-mile delivery fleet managers, when selecting the routes to be covered by different vehicles.

Table 3
Set of proposed scenarios.

	Scenario 1		Scenario 2		Scenario 3		Scenario 4	
Sub-route	v (km/h)	nº stopping elements	v (km/h)	nº stopping elements	v (km/h)	nº stopping elements	v (km/h)	nº stopping elements
1	50	1	50	1	50	1	50	1
2	50	6	30	6	30	4	50	4
3	50	6	50	6	50	6	50	6
4	50	10	30	10	30	8	50	8
5	50	1	50	1	50	1	50	1

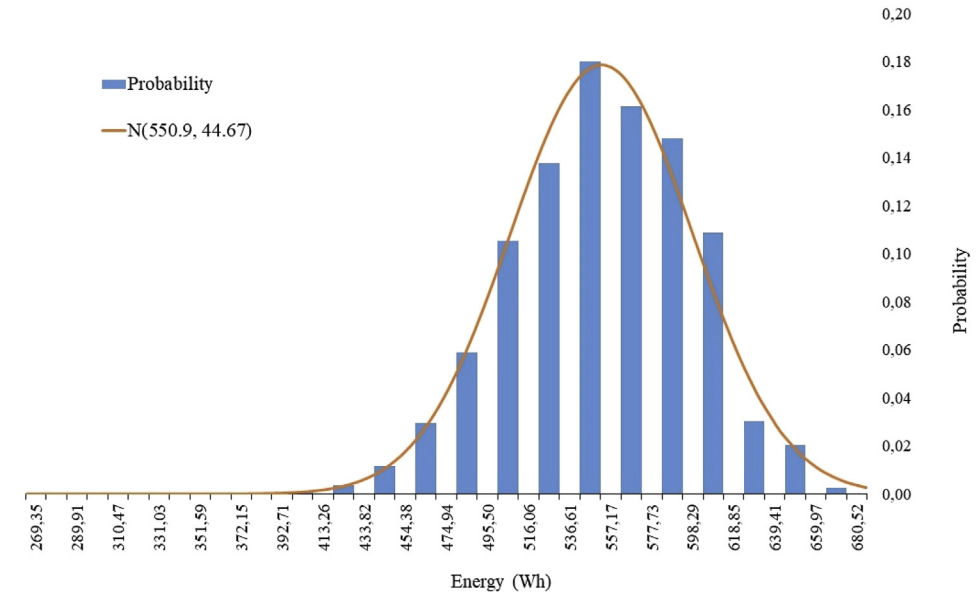

Fig. 7. Probability approximation to a Normal distribution.

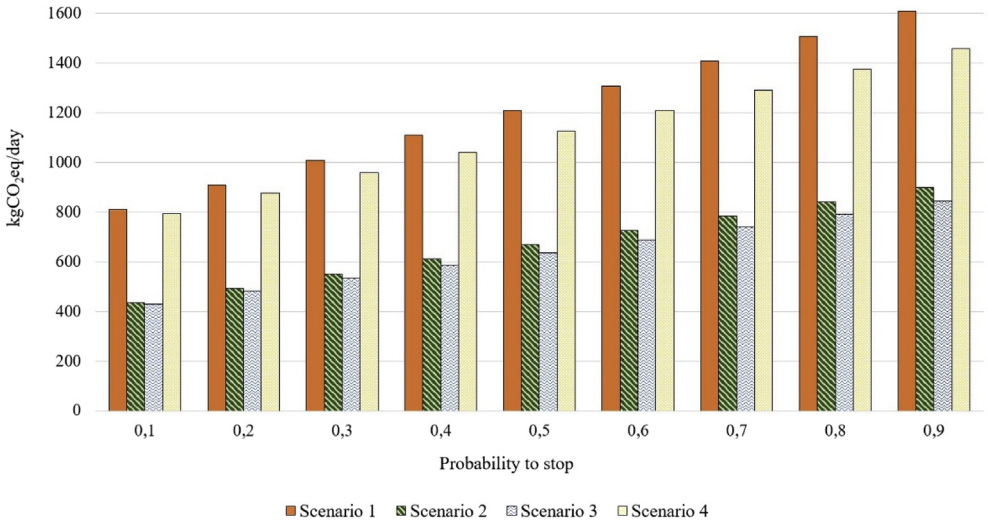

Fig. 8. Results from each scenario.

- Car sharing fleet managers, when selecting and proposing optimal routes.
- Policymakers, when establishing labels to distinguish among different routes and associated emissions, to prioritize future actions.

5. Conclusions and future works

Megacities and their regulations constitute the main barrier for an optimized vehicle (electric or not) to be driven efficiently with minimal emissions. The new models of balanced and sustainable mobility developed in the larger cities are based not only based on the type of fuel used but also on controlling fuel management to optimize consumption and emissions. In this paper, a new methodology has been developed to help control fuel consumption based on the idea that the most important variable, the driver behavior, is conditioned to a set of random and inevitable events that do not actually depends on the driver, but on urban design and traffic control regulations. The influence on consumption of those events has been analyzed from a probabilistic point of view and a reference speed cycle and method for computation have been developed to allow for route characterization. Using this characterization, it is possible to predict the expected energy consumption of an actual vehicle driving an actual route and obeying regulatory constraints.

This method can help policymakers anticipate side effects of policy actions related to BEV users when selecting a route. This paper enhances the transportation of people and goods as part of the production process; therefore if companies need to reduce their environmental impacts, both logistics and commuting routes must be improved to select the optimal (in terms of GHG emissions) fleet composition and to manage vehicles in the most efficient way.

Finally, the authors are aware that although this paper provides a basis for understanding how to quantify urban impact over energy consumption and emissions along a driving route, there is

considerable room for improvement and further investigation. Future research may be oriented in two directions. Firstly, a robust probabilistic model could be constructed by adding more stop events and urban constraints and reinforcing the probabilities assigned to them. One of the first research efforts should focus on linking the method to traffic databases. Secondly, future research should address how to include this perspective into the well-known Vehicle Routing Problem (VRP) and specifically into the Multi-Attribute Vehicle Routing Problem (MAVRP). This may impact the selection of methods used to solve MAVRPs, tipping the balance in favor of heuristics and meta-heuristics algorithms.

References

Aguado, S., Alvarez, R., Domingo, R., 2013. Model of efficient and sustainable improvements in a lean production system through processes of environmental innovation. J. Clean. Prod. 47, 141–148.

Alvarado, H., Batanero, C., 2006. El significado del teorema central del límite: evolución histórica a partir de Sus campos de problemas. In: Investig. en Didáctica las Matemáticas/Congreso Int. sobre Apl. y Desarro. la Teoría las Funciones Semióticas 20.

Alvarez, R., López, A., De la Torre, N., 2015. Evaluating the effect of a driver's behaviour on the range of a battery electric vehicle. Proc. Inst. Mech. Eng. - Part D J. Automob. Eng. 229, 1379–1391. https://doi.org/10.1177/0954407014561483.

Álvarez, R., Zubelzu, S., Díaz, G., López, A., 2015. Analysis of low carbon super credit policy efficiency in European Union greenhouse gas emissions. Energy 82, 996–1010. https://doi.org/10.1016/j.energy.2015.01.110.

Borge, R., Artíñano, B., Yagüe, C., Gomez-Moreno, F.J., Saiz-Lopez, A., Sastre, M., Narros, A., García-Nieto, D., Benavent, N., Maqueda, G., Barreiro, M., de Andrés, J.M., Cristóbal, Á., 2018. Application of a short term air quality action plan in Madrid (Spain) under a high-pollution episode - Part I: diagnostic and analysis from observations. Sci. Total Environ. 635, 1561–1573. https://doi.org/10.1016/j.scitotenv.2018.03.149.

Coelho, M.C., Farias, T.L., Rouphail, N.M., 2005. Impact of speed control traffic signals on pollutant emissions. Transp. Res. D Transp. Environ. 10, 323–340. https://doi.org/10.1016/j.trd.2005.04.005.

Coloma, J., García, M., Wang, Y., Monzón, A., 2017. Green Eco-driving effects in non-congested cities. Sustainability 10 (1), 28.

de Madrid, Ayuntamiento, 2019. Tráfico. Mapa de tramas de intensidad del tráfico - portal de datos abiertos del Ayuntamiento de Madrid [WWW Document]. https://datos.madrid.es/portal/site/egob/menuitem.c05c1f754a33a9fbe4b2e4b284f1a5a0/?vgnextoid=23d57fa19bfa7410VgnVCM2000000c205a0aRCRD&vgnextchannel=374512b9ace9f310VgnVCM100000171f5a0aRCRD. accessed 2.6.19.

DGT, 2018. Distancia de seguridad [WWW Document]. http://revista.dgt.es/es/educacion-formacion/conducir-mejor/2017/1026Distancia-de-seguridad.shtml#.W_P2L3ZRdL0. accessed 7.24.18.

Ehsani, M., Gao, Y., Longo, S., Ebrahimi, K., 2018. Modern Electric, Hybrid Electric, and Fuel Cell Vehicles. CRC press.

ElectricityMap, 2019. ElectricityMap [WWW Document]. https://www.electricitymap.org/?page=country&solar=false&remote=true&wind=false&countryCode=ES. accessed 3.7.19.

Ensslen, A., Paetz, A.-G., Babrowski, S., Jochem, P., Fichtner, W., 2016. On the Road to an Electric Mobility Mass Market—How Can Early Adopters Be Characterized?, pp. 21–51. https://doi.org/10.1007/978-3-319-24229-3_3.

Fathollahi-Fard, A.M., Hajiaghaei-Keshteli, M., 2018. A stochastic multi-objective model for a closed-loop supply chain with environmental considerations. Appl. Soft Comput. 69, 232–249.

Fathollahi-Fard, A.M., Hajiaghaei-Keshteli, M., Tavakkoli-Moghaddam, R., 2018. A bi-objective green home health care routing problem. J. Clean. Prod. 200, 423–443.

Fathollahi-Fard, A.M., Hajiaghaei-Keshteli, M., Mirjalili, S., 2019. A set of efficient heuristics for a home healthcare problem. Neural Comput. Appl. 1–21.

Fernández, R.Á., 2018. A more realistic approach to electric vehicle contribution to greenhouse gas emissions in the city. J. Clean. Prod. 172, 949–959. https://doi.org/10.1016/j.jclepro.2017.10.158.

Ferreira, M., D'Orey, P.M., 2012. On the impact of virtual traffic lights on carbon emissions mitigation. IEEE Trans. Intell. Transp. Syst. 13, 284–295. https://doi.org/10.1109/TITS.2011.2169791.

Fu, Y., Tian, G., Fathollahi-Fard, A.M., Ahmadi, A., Zhang, C., 2019. Stochastic multi-objective modelling and optimization of an energy-conscious distributed permutation flow shop scheduling problem with the total tardiness constraint. J. Clean. Prod. 226, 515–525.

González-Mahecha, R.E., Lucena, A.F., Garaffa, R., Miranda, R.F., Chávez-Rodriguez, M., Cruz, T., Rathmann, R., 2019. Greenhouse gas mitigation potential and abatement costs in the Brazilian residential sector. Energy Build. 184, 19–33.

Govindan, K., Rajendran, S., Sarkis, J., Murugesan, P., 2015. Multi criteria decision making approaches for green supplier evaluation and selection: a literature review. J. Clean. Prod. 98, 66–83.

Greenwood, I.D., Dunn, R.C., Raine, R.R., 2007. Estimating the effects of traffic congestion on fuel consumption and vehicle emissions based on acceleration noise. J. Transport. Eng. 133 (2), 96–104.

Haklay, M., Weber, P., 2008. OpenStreetMap: user-generated street maps. IEEE Pervasive Comput 7, 12–18. https://doi.org/10.1109/MPRV.2008.80.

IDAE, 2018. Plan MOVALT vehículos | IDAE [WWW Document]. https://www.idae.es/ayudas-y-financiacion/para-movilidad-y-vehiculos/plan-movalt-vehiculos. accessed 10.4.18.

IEA. International Energy Agency, 2017. CO_2 Emissions from Fuel Combustion Highlights 2017.

Jones, G.A., Warner, K.J., 2016. The 21st century population-energy-climate nexus. Energy Policy 93, 206–212.

Junquera, B., Moreno, B., Álvarez, R., 2016. Analyzing consumer attitudes towards electric vehicle purchasing intentions in Spain: technological limitations and vehicle confidence. Technol. Forecast. Soc. Chang. 109, 6–14.

Liu, X., Tian, G., Fathollahi-Fard, A.M., Mojtahedi, M., 2019. Evaluation of ship's green degree using novel hybrid approach combining group-fuzzy-entropy and cloud technique for order of preference by similarity to ideal solution theory. Clean Technol. Environ. Policy 1–19.

Lv, C., Zhang, J., Li, Y., Yuan, Y., 2015. Mechanism analysis and evaluation methodology of regenerative braking contribution to energy efficiency improvement of electrified vehicles. Energy Convers. Manag. 92, 469–482. https://doi.org/10.1016/j.enconman.2014.12.092.

Munoz-Organero, M., Ruiz-Blaquez, R., Sánchez-Fernández, L., 2018. Automatic detection of traffic lights, street crossings and urban roundabouts combining outlier detection and deep learning classification techniques based on GPS traces while driving. Comput. Environ. Urban Syst. 68, 1–8. https://doi.org/10.1016/j.compenvurbsys.2017.09.005.

O'Driscoll, R., Stettler, M.E.J., Molden, N., Oxley, T., ApSimon, H.M., 2018. Real world CO2 and NOx emissions from 149 Euro 5 and 6 diesel, gasoline and hybrid passenger cars. Sci. Total Environ. 621, 282–290. https://doi.org/10.1016/j.scitotenv.2017.11.271.

Palat, B., Delhomme, P., Saint Pierre, G., 2014. Numerosity heuristic in route choice based on the presence of traffic lights. Transp. Res. F Traffic Psychol. Behav. 22, 104–112.

Papageorgiou, M., Kiakaki, C., Dinopoulou, V., Kotsialos, A., Wang, Y., 2003. Review of road traffic control strategies. Proc. IEEE 91, 2043–2067. In: https://doi.org/10.1109/JPROC.2003.819610.

Qi, W., Li, L., Liu, S., Shen, Z.-J.M., 2018. Shared mobility for last-mile delivery: design, operational prescriptions, and environmental impact. Manuf. Serv. Oper. Manag. 20, 737–751. https://doi.org/10.1287/msom.2017.0683.

Rauh, N., Franke, T., Krems, J.F., 2015. Understanding the impact of electric vehicle driving experience on range anxiety. Hum. Factors J. Hum. Factors Ergon. Soc. 57, 177–187. https://doi.org/10.1177/0018720814546372.

Renault, 2018. nuevo Renault zoe [WWW Document]. https://www.renault.es/e-brochure/ZOEB10/pdf/fullPDF.pdf. accessed 10.1.19.

Ross, S.M., 2018. Introduction to probability models. In: Options. De Gruyter, Berlin, Boston, pp. xv–xviii. https://doi.org/10.1515/9781547400096-204.

SARTRE consortium, 2004. European Drivers and Road Risk. Part 1. Report on Principle Analyses.

Sepehri, A., Sarrafzadeh, M.H., 2018. Effect of nitrifiers community on fouling mitigation and nitrification efficiency in a membrane bioreactor. Chem. Eng. Processing Process. Intensification 128, 10–18.

She, Z.-Y., Sun, Qing, Ma, J.-J., Xie, B.-C., 2017. What are the barriers to widespread adoption of battery electric vehicles? A survey of public perception in Tianjin, China. Transp. Policy 56, 29–40. https://doi.org/10.1016/j.tranpol.2017.03.001.

Sivak, M., Schoettle, B., 2012. Eco-driving: strategic, tactical, and operational decisions of the driver that influence vehicle fuel economy. Transp. Policy 22, 96–99.

The Commission of the European Communities, 2013. Commission Directive 93/116/EC of 17 December 1993 Adapting to Technical Progress Council Directive 80/1268/EEC Relating to the Fuel Consumption of Motor Vehicles 39–53.

Transport for London. Charges for driving in London. n.d[WWW Document]. https://tfl.gov.uk/modes/driving/charges-for-driving-in-london. accessed 7.4.18.

Woodcock, J., Edwards, P., Tonne, C., Armstrong, B.G., Ashiru, O., Banister, D., Beevers, S., Chalabi, Z., Chowdhury, Z., Cohen, A., Franco, O.H., Haines, A., Hickman, R., Lindsay, G., Mittal, I., Mohan, D., Tiwari, G., Woodward, A., Roberts, I., 2009. Public health benefits of strategies to reduce greenhouse-gas emissions: urban land transport. Lancet 374, 1930–1943. https://doi.org/10.1016/S0140-6736(09)61714-1.

Zubelzu, S., Álvarez, R., 2016. A simplified method to assess the influence of the power generation mix in urban carbon emissions. Energy 115, 875–887. https://doi.org/10.1016/j.energy.2016.09.067.

Glossary

L: Route length
L_v: Length by speed
k: Maximum different speeds number
N_v: Number of stretches
m_v: Stretch type O_1
n_v: Stretch type O_2

t: Stretch type O_3
L_t: Length of transition stretches
R_t: Route
S/S_b: Sub-route
T_{rt}: Transition stretches
p: Number of speed limit changes
M: Vehicle mass
v: Sub-route maximum speed
a: Acceleration
ρ: Air density
C_d: Air resistance coefficient
A: Projected area
g: G-forces
h: Difference of elevation
τ: Rolling resistance coefficient
α: Capacity of the powertrain to recover energy
T: Time of CP_{BEV} stretches
CP_{BEV} *(constant speed):* Consumed energy for stretches type O_1
CP_{BEV} *(acceleration):* Consumed energy for stretches type O_2 during deceleration
CP_{BEV} *(braking):* Consumed energy for stretches type O_2 during acceleration
CP_{BEV} *(transition):* Consumed energy for stretches type O_3
$P(t)$: Power as a function of time
$F(t)$: Force as a function of time
M_s: Row array created with the route characteristics
M_e: Column array created by the energies associated to each stretch
P_i: Probability to not stop.
S_{gr}: Number of stretches that composes the corresponding maximum speed sub-route
PR: Permutations of feasible combinations
$P(A_i)$: Probability of a combination of stretch events
A_i: Combination of stretch events
M_{sbc}: Matrix of energy consumptions and their probabilities
M_{sbr}: Matrix of energy recovered in a sub-route
M_{sb}: Sum of M_{sbc} and M_{sbr}
E_{route}: Route consumption of energy
$P(E_{route})$: Probability of route consumption of energy
$E(NC_{sb})$: Mean of consumed energy of a sub-route
$Var(NC_{sb})$: Variance of a sub-route consumed energy
NC_{sb}: Random discrete variable of consumed energy of a sub-route
NC_{route}: Random discrete variable of consumed energy of a route